NTNU
Norwegian University of Science and Technology

Department of Chemical Engineering

TKP4580 - Chemical Engineering, Specialization Project

Modeling of Offshore Blue Hydrogen Production

Author: Yoonsik Oh

Supervisor: Johannes Jäschke

Co-supervisor: Evren Mert Turan

December 22, 2022

Abstract

Renewable energy is expanding and developing steadily, but not enough. Finding new methods and ways to produce eco-friendly fuels and energy sources is crucial. Hydrogen is one of these potential energy sources. However, the most common way to produce hydrogen is environmentally harmful as it produces a massive amount of CO_2 as a by-product with the hydrogen. There are more low-carbon-emitting ways to produce hydrogen, such as implementing carbon capture and storage. Hydrogen produced with this method is called blue hydrogen. Most blue hydrogen is produced onshore, which requires a lot of transporting gases back and forth as natural gas needs to be transported onshore, and the captured CO_2 needs to be transported back offshore where it is stored. Moving this process offshore (platform or ship) drastically reduces the need for transport, as the hydrogen product is the only transport back onshore. The process also needs to be modified as there are more limiting constraints for weight and space when operating offshore. Studying feasibility requires a model that describes the process as close to reality as possible, which is this project's final goal.

The optimization results will be studied to evaluate the model after formulating the optimization problem and if the simulation found a feasible solution to conclude the model as finalized. Then the finalized model will be used to simulate sensitivity analysis cases to evaluate how the system reacts to different inputs, in other words, the robustness of the model. Results show good numbers as it converts all natural gas into only CO_2, H_2O, and hydrogen, with a 99.6% conversion rate. By implementing already known methods for capturing CO_2, at least 95% of the CO_2 emissions from the process are captured. The sensitivity analysis shows that the model runs stably, and the output is insensitive when varying inputs. This almost-fully tested model will be used when implementing a robust control structure that ensures a maximum profit or minimal energy cost for disturbances. Further work may include implementing more accurate post-conversion separation factors, robust plantwide control, sizing, and economical analysis.

Contents

List of Figures

List of Tables

1 Introduction

1.1 Background and motivation

The world desperately needs a new energy solution as the global energy demand has a steady pace of growth. Since 1900, the demand has risen by 2.8% each year and a growth of 2.2% in the 21st century[2]. A statistical review of world energy from BP shows that in 2021, over 83% of the world's energy consumption comes from fossil fuel sources[3]. This shows that the global infrastructure is heavily dependent on energy generated on CO_2 emitting sources. Even though the EU has set a climate-neutral goal by 2050, the shift rate is not enough[4]. In 2018, wind and solar energy sources produced around 1850TWH per annum globally, while their peak annual growth is around 130-140TWH per annum. With this rate, it would take around 180 years only to meet 50% of the global energy demand in 2050[2]. Electricity generated from various renewable energy sources such as hydro power, windmills, and solar panels is not enough to replace the huge demand for energy that the current global infrastructure requires[2]. Among the important research and development areas for clean and alternative energy, hydrogen is one of the promising alternatives.

Hydrogen is viewed as an important energy carrier for the decarbonized future and is already widely used for various purposes around the world and the industry. Hydrogen has also potentially an important role in three major global energy crisis issues[5]. The first one is to supply clean fuel to meet the demand for liquid and gaseous fuels and electricity, as hydrogen is considered a fuel source without greenhouse gas emissions, as the only emission is water vapor in a fuel cell. The second is to increase energy utilization efficiency for fuels and electricity production. The third is to tackle the issue of pollutants, and the link between energy utilization and greenhouse gas emission in end-use systems[5].

Even though hydrogen in a fuel cell is emission-free, it is indirectly associated with the related environmental effects and CO_2 emissions from the method of producing it. The most common way to commercially produce hydrogen is by steam-methane reforming. By reacting methane with a high-temperature stream under 3-25 bar pressure in the presence of a catalyst, hydrogen atoms are separated from carbon atoms in methane[6]. Hydrogen produced by this process is called "grey hydrogen". Hydrogen can also be produced by electrolysis, which is a process that splits hydrogen from water using an electric current. Hydrogen produced by electrolysis is called "green hydrogen". Hydrogen produced by steam-methane reforming where the majority of the CO_2 is captured and stored (CCS) is called "blue hydrogen".

Almost 96% of all hydrogen production globally is generated from fossil fuels, mostly from steam-methane reforming and coal gasification. Blue hydrogen is a relatively new concept, and as of 2021, two blue hydrogen facilities produce hydrogen at a commercial scale in North America[7]. These facilities are based on land, as most natural gas in North America is also extracted on land. But when implementing this technology in Norway, natural gas is extracted from the sea, which is far from land. To implement the same blue hydrogen, it requires the natural gas to be transported onshore, where the gas is processed, CO_2 is

captured and transported back to the offshore platform, where the CO_2 gas is stored in the oil reservoir where the natural gas originated from.

This project will look at the feasibility of an offshore blue hydrogen production where the natural gas from the oil reservoir will be extracted and reformed into hydrogen and CO_2 gas on the same unit, either on a ship or a platform. The CO_2 will be captured on the same unit, transported, and stored in the same oil reservoir where the natural gas was extracted. The hydrogen gas will be transported to an onshore plant. Suppose such a plant is feasible, where clean hydrogen can be produced without large amounts of emissions. In that case, it can play a crucial role in meeting the future global energy demand and decarbonizing the future.

This project is a part of the SUBPRO Zero Blue Hydrogen project. SUBPRO is a center in Research-based innovation (SFI) within subsea production and processing and is cooperating with different oil and gas industries in Norway [8]. Much research is needed to study if a project of this scale is feasible. There is the model feasibility and the economic feasibility. The goal is to develop the existing steady-state model at SUBPRO by testing its sensitivity and robustness. When the model is tested to be feasible and robust, it can be further used to study the economic feasibility.

In the report, theory around the process and optimization will be presented, and how the system and the model are built. The model will be optimized for each implementation made with a simple objective function, and the resulting variables will be observed and studied for each optimization. Lastly, the results will be presented and discussed before concluding the project.

1.2 Scope of the project

In this section, the scope of the project will be discussed, in other words, what aspects to focus on and whatnot. This project aims to develop an existing model by SUBPRO, as the existing model is still under development. The choice of the process was decided in the existing model that was developed at SUBPRO, so the scope of this project would not consider the choice of process. Different aspects will be implemented in the process, such as more accurate oxygen combustion reactions in the reactor and heat exchanging physics in the reactors. The model will not take the physics, and the complexity behind the transport and storage of CO_2 and will only be focusing on improving the model without not considering what is happening with the product outflow.

2 Theory

2.1 Introduction to Optimization

Optimization is an important mathematical tool when analyzing a system. First, an objective function needs to be identified/defined. This objective function could, for example, be either profit or energy required. The objective function will depend on variables; the goal is to find the best variables that either minimize or maximize the objective function within an allowed set. This set is defined by different constraints and can be compared to a domain where the function can be.

A typical minimizing optimization problem can be defined as

$$\min_{x \in \mathbb{R}^n} f(x) \tag{2.1.1}$$

$$\text{s.t.} \quad c_i(x) = 0, \quad i \in \mathcal{E} \tag{2.1.2}$$

$$c_i(x) \leq 0, \quad i \in \mathcal{I}, \tag{2.1.3}$$

where x is the vector of decision variables, $f(x)$ is the objective function, $c_i(x)$ is the constraint functions, $\mathcal{E}$ and $\mathcal{I}$ are the sets of indices for equality and inequality constraints, respectively. Once the optimization problem has been defined, the next step is to choose the optimal optimization algorithm to solve the problem. No universal algorithm is the best for all cases, but there is a collection of algorithms tailored to different problems. The responsibility of choosing the best algorithm often falls to the user. It is important to choose the best algorithm given the problem as the solving time will heavily depend on the algorithm and whether the algorithm can find a solution at all[9]. To ensure that the solution found by the algorithm is the real solution, some conditions need to hold for the solution to be concluded as the true solution. These conditions are defined in appendix A.

2.2 Conservation laws

In general, conservation laws state that a certain quantity does not change over time as long as the system is closed or does not interact with its environment in any way. A steady-state assumption has been made. In other words, there is no accumulation. The general balance equation can be described as follows:

$$\text{Accumulation} = \text{Input} - \text{Output} + \text{Generation}, \tag{2.2.1}$$

or described mathematically:

$$0 = \sum x_{in} - \sum x_{out} + \sum x_{gen}, \tag{2.2.2}$$

where the left-hand side of eq. (2.2.2) is the change of the quantity, x, in the system, and the terms on the right-hand side are the quantity inlet streams, quantity outlet streams, and generated quantity, respectively. If there is no chemical reaction, x_{gen} is usually zero. Also, in a steady-state system, the left-hand side term is zero.

2.2.1 Mass balance

The law of conservation of mass states that mass cannot be created or destroyed in a process in a closed system. By using the general balance equation from eq. (2.2.2), with the assumption of steady-state, the general mass balance equation will be described as

$$0 = \sum m_{in} - \sum m_{out} + 0 \tag{2.2.3}$$

$$\sum m_{in} = \sum m_{out}, \tag{2.2.4}$$

where $\frac{d}{dt} = 0$, and $\sum x_{gen} = 0$, due to steady-state assumption and mass can not be generated nor destroyed. In other words, the sum of all inlet mass streams must be equal to that of all outlet mass streams. It is important to ensure that eq. (2.2.4) holds for every process inventory as it ensures that there is no model mismatch. Some deviation is expected when using a computer to solve problems due to machine precision.

2.2.2 Component balance

When defining balance equations for components in the system, it is typically done by balancing the moles of each component. From the general balance equation (eq. (2.2.2)), the general component balance is defined as

$$0 = n_{i,in} - n_{i,out} + G_i, \tag{2.2.5}$$

where i is a component in the system, $n_{i,in}$ is the inlet mole stream of component i, $n_{i,out}$ is the outlet mole stream of component i and $\dot{G}_i$ is the generated mole of component i and describes the reaction in the system. When considering the system as a steady-state system, the component balance can be described as

$$n_{i,out} = n_{i,in} + G_i. \tag{2.2.6}$$

The generated mole of component i can be described as

$$G_i = \sum_j \nu_{i,j}\xi_j, \tag{2.2.7}$$

where $\nu_{i,j}$ is the stoichiometric coefficient for component i in reaction j and ξ_j is the extent of reaction for reaction j[10]. By combining eq. (2.2.6) and eq. (2.2.7), the final general component balance is then defined as

$$n_{i,in} = n_{i,out} + \sum_j \nu_{i,j}\xi_j. \tag{2.2.8}$$

2.2.3 Energy balance

The law of conservation of energy states that energy cannot be created or destroyed; in other words, the total energy in a system stays constant. However, it can be transformed or transferred from one form to another. The general energy balance is given as

$$0 = E_{in} - E_{out} + Q + W, \tag{2.2.9}$$

where E_{in} and E_{out} are the energy added and removed from the system from the mass streams, Q and W are the added or removed heat and work to the system from the environment, respectively. Total energy, E, is defined as the sum of internal energy, kinetic energy, and potential energy, or

$$E = U + E_k + E_p \tag{2.2.10}$$

For a typical process, kinetic and potential energy can be assumed to be neglected[11]. Then $E = U$, and with the assumption of a steady-state process, the energy balance becomes

$$0 = U_{in} - U_{out} + Q + W, \tag{2.2.11}$$

where U_{in} and U_{out} are the internal energy of the inlet and outlet mass streams, respectively. The W term is a sum of various work contributions such as flow, mechanical, and electrochemical, but in this project, only flow work will be considered, such that $W = W_{flow}$. W_{flow} is defined as:

$$W_{flow} = W_{flow,in} - W_{flow,out} \tag{2.2.12}$$

$$= p_{in}V_{in} - p_{out}V_{out}. \tag{2.2.13}$$

Introducing the definition of enthalpy as the sum of internal energy and flow work:

$$H = U + pV \tag{2.2.14}$$

By combining eq. (2.2.11), eq. (2.2.13) and eq. (2.2.14), the final energy balance is defined as

$$U_{out} = U_{in} + Q + W_{flow} \tag{2.2.15}$$

$$U_{out} = U_{in} + Q + p_{in}V_{in} - p_{out}V_{out} \tag{2.2.16}$$

$$U_{out} + p_{out}V_{out} = U_{in} + p_{in}V_{in} + Q \tag{2.2.17}$$

$$H_{out} = H_{in} + Q. \tag{2.2.18}$$

2.3 Flowsheet modeling

To investigate the impacts of disturbances, proposed control strategies, start-ups, and shutdowns of a real plant, a flowsheet model, can be used to simulate a plant-wide operation. When the model is sufficiently validated through various analyses, such as sensitivity analysis, it can be used as PAT (process analytical technology) in the real system. This model can then substitute expensive real physical PAT and implement advanced process control such as an MPC (model predictive control) or dynamic optimization. The general idea with flowsheet modeling is to construct a process diagram, which can simulate different cases once the correct operating parameters have been defined. In other words, flowsheet models can be used to communicate through a graphical user interface with the user to explain the process[12].

There are two main ways to set up a flowsheet model. There is a sequential approach and a simultaneous approach. The sequential approach connects subunit models with their own

procedures for the solution to pass information upstream and downstream so that the outlet material and enthalpy flow becomes the inputs for the subunit to explain how the actual process plant works[12]. The simultaneous approach will have the same connection where the subunits are bound to each other through connectivity constraints, where one subunits outlet information is the connected subunits inlet information, but all the subunits will be solved simultaneously.

There are both pros and cons to both approaches. The advantage of the sequential approach is that it will be easier to identify potential errors, both model mismatch and numerical errors. The disadvantage is that optimizing a sequential modular flowsheet will be more difficult as the subunits usually provide the variables as results and not the gradients needed for efficient optimization for some first and second-order methods. On the contrary, the advantage of a simultaneous approach is that it can solve a system with recycle loops or energy exchange between units, while a sequential approach may cause non-conversion. The disadvantage is that there is harder to identify potential errors in the model. And also, in a simultaneous approach, it will be harder to initialize the simulator as good initial guesses for the whole system may be needed to find a solution.

3 Process Description

Even though many ways are well studied for blue hydrogen production, there are other circumstances when designing such a plant offshore, as there are limiting constraints for space and weight, and the building cost will be higher. An ordinary blue hydrogen production plant uses a large furnace to perform the steam-methane reforming, which takes up a lot of space. The columns can not be too high because the waves will sway the ship. Instead of relying on a regular steam-methane reformer, the project will depend on a method from the company *Johnson Matthey* has designed. This method replaces the large furnace with an autothermal reformer (ATR) combined with the gas-heated reformer (GHR) with pure oxygen stream into the ATR. This method has reported high hydrogen purity with a low carbon emission[13]. A detailed description of the process will be broken down into parts and described in the following subsection. Extracted natural gas will enter the process, and hydrogen will be produced. The by-product CO_2 will be captured and transported back to the reservoir. The hydrogen product will be transported onshore and used for various purposes. A simplified figure of this process can be shown in fig. 1.

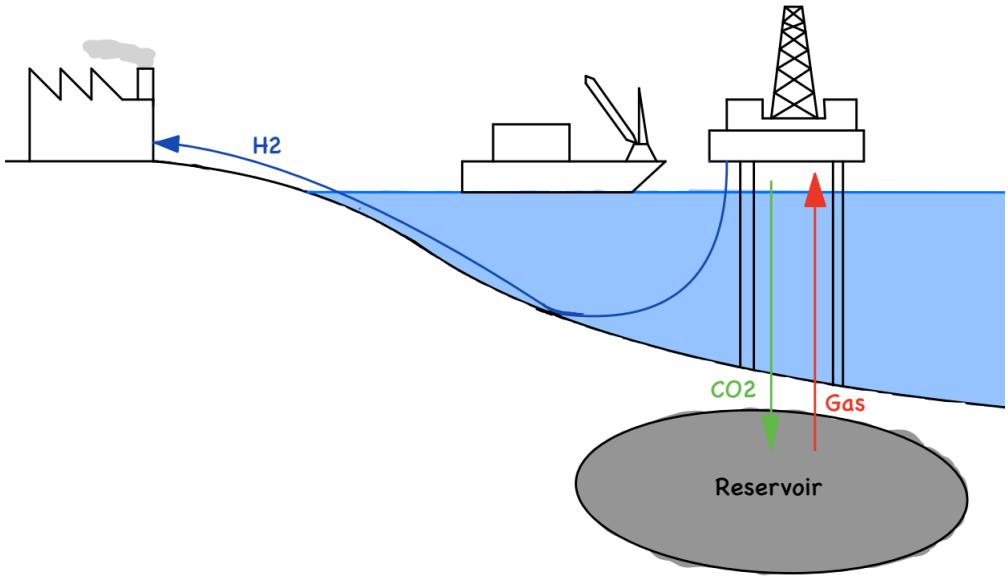

Figure 1: Simplified model of the offshore blue hydrogen process.

3.1 Flowsheet

3.1.1 Feed stream

The complete flowsheet on which the modeling in this project takes basis is shown in fig. 2. The feed stream, or stream 1, is the natural gas extracted from the North Sea oil and gas reservoir. It consists mainly of methane, CO_2, and other heavier organic compounds like ethane and propane. It also has traces of other inorganic compounds like sulfuric and nitric compounds. The model assumes that all heavier hydrocarbons than pentane will be

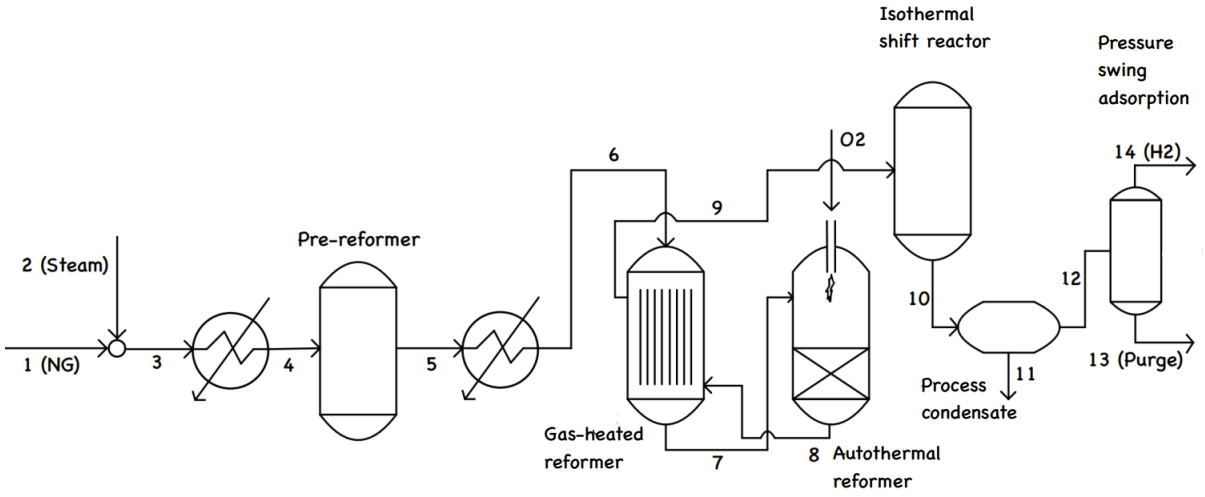

Figure 2: Flowsheet of the process used in the model.

considered as pentane, C_5H_{12}. The composition of stream 1 is set to be identical to an average composition from a typical natural gas in the North Sea[1]. An assumption that all nitrous and sulfuric compounds are removed has been made, and the remaining mole% is assumed to be CH_4. Sulphuric compounds are removed by adding hydrogen to the natural gas stream, which will convert all sulfuric components to H_2S, which is removed. This is important as even though there are only traces of sulfuric compounds, sulfur is often the leading cause of catalyst damage in the reactors, which causes a loss in profit and yield in the product stream. A table of the composition of different compounds used as initial values in the model is shown in table 1.

Table 1: Average composition of natural gas in the north sea.[1]

Compound	%mol
CH_4	78.27
C_2H_6	6.10
C_3H_8	6.70
n-C_4H_{10}	2.48
i-C_4H_{10}	1.41
C_5H_{12}	3.70
H_2O	≈ 0
H_2	≈ 0
CO	≈ 0
CO_2	1.34
H_2S	≈ 0

3.1.2 Pre-reformer

The purified natural gas stream (stream 1) will be mixed with steam (stream 2). Its purpose is to saturate the natural gas stream with steam for different stages later, like pre-reforming, methane steam reforming, and water gas shift reaction. The steam amount is set to a steam-to-carbon ratio of 2.5, where carbon is the sum of all the hydrocarbons in the inlet stream. A steam-to-carbon ratio of 2.5 is typical for hydrogen production in an adiabatic pre-reformer[14]. The saturated, purified natural gas stream (stream 3) will enter a heater before entering the first reactor, the pre-reformer. The outlet temperature of the heater is set to be 693.0 K, which is a good low operating temperature for the pre-reformer[14]. The pre-reformers task is to convert all the heavier hydrocarbons into methane. Due to the reactor conditions, it is assumed that the first equilibrium, shown in eq. (3.1.1), is heavily shifted towards the right. The second equilibrium, shown in eq. (3.1.2), is heavily shifted towards the left due to the reactor conditions such that all heavy hydrocarbons convert to methane. These equilibrium equations are also called the steam reforming equations[15]. To meet the reactor conditions, the inlet stream is heated before the pre-reformer. In summary, in the pre-reformer step, hydrocarbons and water are being converted to CO and H_2, and CO and H_2 will convert back to methane and water.

$$C_nH_m + nH_2O \rightleftharpoons nCO + (n + m/2)\,H_2, \quad \Delta H > 0 \tag{3.1.1}$$

$$CH_4 + H_2O \rightleftharpoons CO + 3\,H_2, \quad \Delta H > 0 \tag{3.1.2}$$

3.1.3 Gas heated reformer and Autothermal reformer

After the pre-reformer step, stream 5 will enter a heater to set the stream temperature to 753.0 K. A temperature of 923 K to 1023 K is the operating temperature for the gas heater reformer, which is a good operating temperature range to achieve near equilibrium and produces hydrogen-rich gas[15]. Since this model takes the steady-state assumption, the reactor will be at equilibrium. The heated stream will enter the second reactor, R2, which is the gas-heated reformer (GHR). The GHR consists of catalyst-filled pipes where the inlet stream passes through, and two reactions, steam methane reforming and water gas shift reaction will take place. These equations are shown in eq. (3.1.2) and eq. (3.1.3). The outlet of the GHR will enter the next reactor, R3, which is the autothermal reformer (ATR). In the ATR, a stream of pure oxygen is fed into the reactor such that the heat from combusting oxygen gives higher conversion of H_2 and CO_2 since the reaction is endothermic (eq. (3.1.2)). Oxygen can combust with mainly two components; methane and hydrogen. It is found from a study that hydrogen burns with oxygen ten times faster than methane[16]. Due to this reason, it is assumed that the oxygen will only combust with hydrogen, and the methane combustion will not be modeled.

The GHR is designed such that the outlet of the ATR is exchanging heat with the pipelines in the GHR. This is preferred as the heat from the ATR is high, and the outlet from ATR can exchange a satisfying amount of heat such that the reactions occurring in the pipelines

in the GHR give greater conversion of H_2 and CO from eq. (3.1.2). This heat exchange is similar to a tube and shell heat exchanger. After the ATR and GHR process, almost all methane has converted, and the outlet stream will mainly consist of CO, CO_2, H_2O, and hydrogen.

$$CO + H_2O \rightleftharpoons CO_2 + H_2, \quad \Delta H < 0 \tag{3.1.3}$$

3.1.4 Isothermal shift reactor

Stream 9 will then enter the last reactor, R4, which is the isothermal shift reactor (ITSR). The purpose of this step is to convert CO into H_2 and CO_2 to a maximum achievable amount. Due to the catalysts and other conditions like constant temperature in the ITSR, only the water-gas shift reaction, shown in eq. (3.1.3), will occur. As the temperature in the reactor is constant (isothermal) and the reaction happening in the reactor is exothermic, heat is recovered in this part. A typical isothermal shift reactor is operating in a temperature range of 473 K - 623 K with a copper-zinc-alumina catalyst [17]. The outlet stream of ITSR (stream 10) will now mainly consist of H_2O, CO_2, and H_2.

3.1.5 Process condensate

Stream 10 will enter a cooler, bringing the stream's temperature down to 313 K. This leads to the condensation of H_2O so that it can be removed in the process condensate (C3). This part is one of the simpler and cheaper options for post-combustion separation technique [18]. The outlet stream of the process condensate will now mainly consist of H_2 and CO_2. The water removed from the process condensate can be recycled for stream 2 after heating.

3.1.6 Pressure Swing Adsorption

The last step is pressure swing adsorption (PSA). When operating at high pressure, CO_2 is being adsorbed by particles, and H_2 is passed through. When lowering the pressure, CO_2 is desorbed from the particles by flushing it with pure H_2. This technique is similar to a batch reactor, where the process needs to wait until the tank has a saturated amount of CO_2 adsorbed particles and then lower the pressure to flush it out. To model this to a more continuous process, PSA consists of two tanks, where one tank adsorbs with high pressure while the other lower pressure and desorbs the particles [19]. Stream 14 is the product hydrogen stream, which is reported to have a high purity [20], while stream 15 is the CO_2 stream with other unreacted components and other impurities which is being transported back to the reservoir to complete the enhanced oil recovery [21]. The high H_2 purity stream will be transported back onshore, where it can be applied for different purposes.

4 Model Description

When modeling the process, several assumptions were made in addition to the ones explained in section 3.1. The first and most important one is that the model is assumed to be in a steady-state. In other words, no dynamics were implemented. This is to simplify the model when developing and testing the model. The constraints in the optimization problem are formulated as nonlinear algebraic equations. The composition in the inlet stream is assumed to be the same from table 1. To estimate the size of the initial mole stream, natural gas stream data from *Norsk Petroleum* was used, where the platform *Troll* in the North Sea was chosen as it has the largest gas producer in the last decade[22]. *Troll* is producing an average of 35 million Sm^3/year, which is calculated to approximately 4000 Sm^3/h. When converting from unit Sm^3 to kg, the density is estimated to be 0.829 kg/Sm^3. The final initial mole stream was then calculated as 145.4 kmol h^{-1}.

To model the heat exchange connection between the catalyst-filled pipelines in the GHR and the outlet of the ATR, a new variable, Q_{GHR}, is introduced into the GHR when in reality, the GHR as a whole is adiabatic. Then a new additional cooler after ATR is introduced to cool down the outlet stream from ATR. The heat released from the cooler is modeled to be the same as a new Q_{GHR} variable, which is the heat GHR receives from the ATR. The temperature of the stream after the cooler is modeled to be the same as the outlet temperature of the ATR in the flowsheet shown in fig. 2. The new flowsheet, which the model takes basis, is shown in fig. 3.

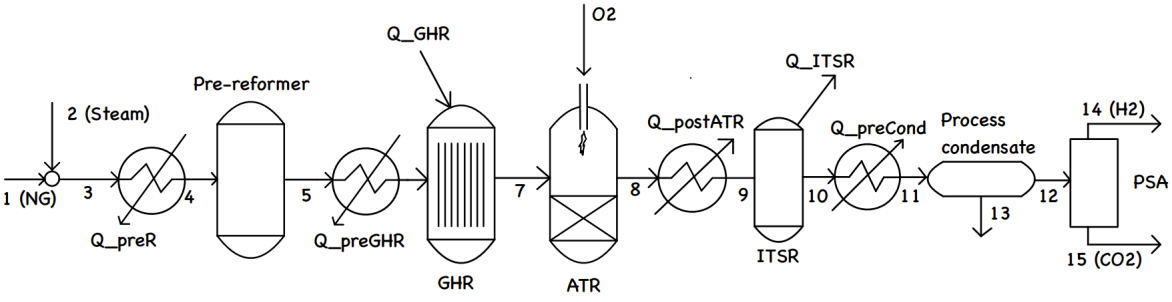

Figure 3: Flowsheet of the process used in the model.

4.1 JuMP Julia Model Structure

To build the model in JuMP Julia, there were first created 11 subunits, which were assembled into a final model at the end. Each subunit is a control volume of the process. After the 11 subunits were assembled, connectivity constraints were added to implement a connection between the flows of each subunit, and initial values. Then the assembled model is solved in a simultaneous approach, where all the subunits are part of a bigger model. Furthermore, a function to print out the mole stream table, other relevant variables, a mass stream table to check that the mass balance is satisfied for every part of the process and a composition table has been made. A summary of the description of each model is shown in table 2.

Ipopt interfaced by JuMP in Julia was used to solve the problem and is an interior point method[23] [24]. In the end, there are a total of 183 variables with 184 constraints, where 2 constraints were inequality constraints. This gives 1 degree of freedom, which is used for the objective function. The objective function is to maximize hydrogen production.

Table 2: Summary of the description of all models.

Model	Inlet	Outlet	What
1Mix.jl	n_1, n_2	n_3	Mixer for streams 1 and 2 and calculate the required amount of steam
2PrePR.jl	n_3	n_4	Heater before pre reformer
3PR.jl	n_4	n_5	Pre reformer
4PreGHR.jl	n_5	n_6	Heater before GHR
5GHR.jl	n_6	n_7	Gas heated reformer
6ATR.jl	n_7	n_8	Autothermal reformer
7PostATR.jl	n_8	n_9	Cooler after ATR
8ITSR.jl	n_9	n_{10}	Isothermal shift reactor
9PreCondensate.jl	n_{10}	n_{11}	Cooler before process condensate
10Condensate.jl	n_{11}	n_{12}, n_{13}	Process condensate
11PSA.jl	n_{12}	n_{14}, n_{15}	Pressure swing adsorption

In general, each subunit first defines the variables with lower bounds and looping through the variables to give each variable an initial value when optimizing. The reactors have their own unique mass balance, but the rest of the subunit models are either heaters, coolers, or stream splitters. The general component balance and energy balance are eq. (2.2.8) and eq. (2.2.18), respectively.

4.1.1 Pre-reformer

The equations in the PR.jl subunit, which is the model for the pre-reformer, are derived from eq. (3.1.1), eq. (3.1.2) and eq. (3.1.3). It is assumed that all heavier hydrocarbons than 5

carbons, will be considered pentane. The equilibrium equations in the pre-reformer are then

$$\mathrm{CH_4 + H_2O \rightleftharpoons CO + 3\,H_2} \tag{4.1.1}$$
$$\mathrm{C_2H_6 + 2\,H_2O \rightleftharpoons 2\,CO + 5\,H_2} \tag{4.1.2}$$
$$\mathrm{C_3H_8 + 3\,H_2O \rightleftharpoons 3\,CO + 7\,H_2} \tag{4.1.3}$$
$$\mathrm{i\text{-}C_4H_{10} + 4\,H_2O \rightleftharpoons 4\,CO + 9\,H_2} \tag{4.1.4}$$
$$\mathrm{n\text{-}C_4H_{10} + 4\,H_2O \rightleftharpoons 4\,CO + 9\,H_2} \tag{4.1.5}$$
$$\mathrm{C_5H_{12} + 5\,H_2O \rightleftharpoons 5\,CO + 11\,H_2} \tag{4.1.6}$$
$$\mathrm{CO + H_2O \rightleftharpoons CO_2 + H_2}. \tag{4.1.7}$$

Assuming all hydrocarbons heavier than methane are shifted heavily towards the right, the extent of the reaction for each reaction can be calculated from the initial mole of the component in the reaction since the final mole of the component is zero. For ethane, the component balance will be

$$0 = n_{0,\mathrm{C_2H_6}} - n_{\mathrm{C_2H_6}} - \xi_{1,pr}, \tag{4.1.8}$$

where $n_{0,\mathrm{C_2H_6}}$ and $n_{\mathrm{C_2H_6}}$ are the inlet and outlet mole of ethane and $\xi_{1,pr}$ is the extent of reaction for eq. (4.1.2) in the pre-reformer. With the assumption that all ethane has reacted, $n_{\mathrm{C_2H_6}} = 0$, then the mole balance becomes:

$$0 = n_{0,\mathrm{C_2H_6}} - 0 - \xi_{1,pr} \tag{4.1.9}$$
$$\xi_{1,pr} = n_{0,\mathrm{C_2H_6}}. \tag{4.1.10}$$

The same method can be used for eq. (4.1.3) to eq. (4.1.6) such that:

$$\xi_{2,pr} = n_{0,\mathrm{C_3H_8}} \tag{4.1.11}$$
$$\xi_{3,pr} = n_{0,\mathrm{i\text{-}C_4H_{10}}} \tag{4.1.12}$$
$$\xi_{4,pr} = n_{0,\mathrm{n\text{-}C_4H_{10}}} \tag{4.1.13}$$
$$\xi_{5,pr} = n_{0,\mathrm{C_5H_{12}}}. \tag{4.1.14}$$

The remaining extent of reactions in the pre-reformer can be obtained from the component balance of methane and CO_2, or eq. (4.1.1) and eq. (4.1.7), respectively. The component balance equations are shown in eq. (4.1.15) and eq. (4.1.16).

$$0 = n_{0,\mathrm{CH_4}} - n_{\mathrm{CH_4}} - \xi_{6,pr} \tag{4.1.15}$$
$$0 = n_{0,\mathrm{CO_2}} - n_{\mathrm{CO_2}} + \xi_{7,pr}. \tag{4.1.16}$$

Then the extent of reaction for eq. (4.1.1) and eq. (4.1.7) are then

$$\xi_{6,pr} = n_{0,\mathrm{CH_4}} - n_{\mathrm{CH_4}} \tag{4.1.17}$$
$$\xi_{7,pr} = n_{\mathrm{CO_2}} - n_{0,\mathrm{CO_2}}. \tag{4.1.18}$$

It is worth noting that all equations for the extent of reactions in the model are explicit expressions in the model and are not calculated by the solver. The reactions shown in eq. (4.1.1) and eq. (4.1.7) are at equilibrium and are not assumed to be shifted heavily

towards the right. The equilibrium constants for these equations describe the ratio between the reactants and product moles after the equilibrium and are dependent on temperature. The equations for the equilibrium constants for eq. (4.1.1) and eq. (4.1.7) are shown in eq. (4.1.19) and eq. (4.1.20), respectively.

$$K_{SMR}(T) = \frac{x_{\mathrm{CO}} \cdot x_{\mathrm{H_2}}^3}{x_{\mathrm{CH_4}} \cdot x_{\mathrm{H_2O}}} \tag{4.1.19}$$

$$K_{WGSR}(T) = \frac{x_{\mathrm{CO_2}} \cdot x_{\mathrm{H_2}}}{x_{\mathrm{CO}} \cdot x_{\mathrm{H_2O}}}, \tag{4.1.20}$$

where $K_{SMR}(T)$ and $K_{WGSR}(T)$ are the temperature-dependent equilibrium constants for the steam-methane reforming and water-gas shift reaction, respectively. The functions for equilibrium constants for both reactions were found by simulating a GHR reactor in the software Aspen HYSYS, where the equilibrium constant was calculated for a temperature range of 700-1300K, and a logarithmic equilibrium constant was estimated with linear regression. The regression plot is shown in fig. 4, and the equation for equilibrium constant for steam-methane reforming and water gas shift reactions are shown in eq. (4.1.21) and eq. (4.1.22), respectively.

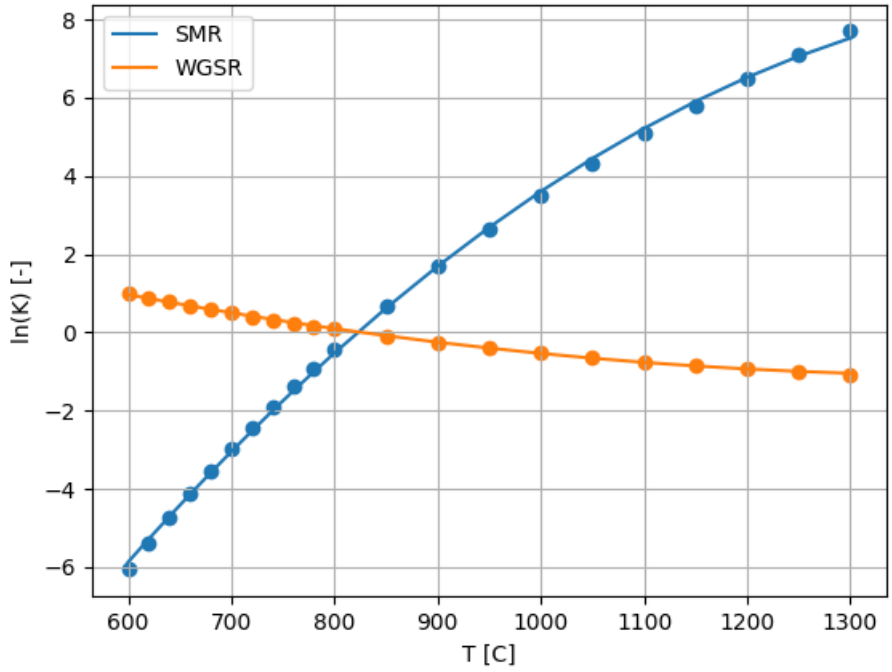

Figure 4: The linear regression for estimating the equations eq. (4.1.21) and eq. (4.1.22) for the equilibrium constants K_{SMR} and K_{WGSR}, respectively.

$$K_{SMR}(T) = \exp\left(-1.52 \cdot 10^{-5} T^2 + 4.80 \cdot 10^{-2} T - 29.19\right) \tag{4.1.21}$$

$$K_{WGSR}(T) = \exp\left(-2.95 \cdot 10^{-6} T^2 - 8.47 \cdot 10^{-3} T - 4.99\right) \tag{4.1.22}$$

With the energy balance equation defined in eq. (2.2.18), component balance equations, and equilibrium constant equation, the equations in the pre-reformer model can be summarized as:

$$0 = n_{0,\mathrm{H_2O}} - n_{\mathrm{H_2O}} - 2\xi_{1,pr} - 3\xi_{2,pr} - 4\xi_{3,pr} - 4\xi_{4,pr} - 5\xi_{5,pr} - \xi_{6,pr} - \xi_{7,pr} \tag{4.1.23}$$

$$0 = n_{0,\mathrm{H_2}} - n_{\mathrm{H_2}} + 5\xi_{1,pr} + 7\xi_{2,pr} + 9\xi_{3,pr} + 9\xi_{4,pr} + 11\xi_{5,pr} + 3\xi_{6,pr} + \xi_{7,pr} \tag{4.1.24}$$

$$0 = n_{0,\mathrm{CO}} - n_{\mathrm{CO}} + 2\xi_{1,pr} + 3\xi_{2,pr} + 4\xi_{3,pr} + 4\xi_{4,pr} + 5\xi_{5,pr} + \xi_{6,pr} - \xi_{7,pr} \tag{4.1.25}$$

$$0 = K_{SMR}(T)(x_{\mathrm{CH_4}} \cdot x_{\mathrm{H_2O}}) - (x_{\mathrm{CO}} \cdot x_{\mathrm{H_2}}^3) \tag{4.1.26}$$

$$0 = K_{WGSR}(T)(x_{\mathrm{CO}} \cdot x_{\mathrm{H_2O}}) - (x_{\mathrm{CO_2}} \cdot x_{\mathrm{H_2}}) \tag{4.1.27}$$

$$0 = n_{0,\mathrm{C_2H_6}} - n_{\mathrm{C_2H_6}} - \xi_{1,pr} \tag{4.1.28}$$

$$0 = n_{0,\mathrm{C_3H_8}} - n_{\mathrm{C_3H_8}} - \xi_{2,pr} \tag{4.1.29}$$

$$0 = n_{0,\text{i-}\mathrm{C_4H_{10}}} - n_{\text{i-}\mathrm{C_4H_{10}}} - \xi_{3,pr} \tag{4.1.30}$$

$$0 = n_{0,\text{n-}\mathrm{C_4H_{10}}} - n_{\text{n-}\mathrm{C_4H_{10}}} - \xi_{4,pr} \tag{4.1.31}$$

$$0 = n_{0,\mathrm{C_5H_{12}}} - n_{\mathrm{C_5H_{12}}} - \xi_{5,pr} \tag{4.1.32}$$

$$0 = \sum_i n_{i,in} \cdot h_i(T_{in}) - \sum_i n_{i,out} \cdot h_i(T_{out}) + Q_{PR}, \tag{4.1.33}$$

where eq. (4.1.33) is obtained from eq. (2.2.18) by defining H_{in} and H_{out} as the sum of each component mole in the stream multiplied by the specific enthalpy of the component at the given temperature, either inlet or outlet temperature.

4.1.2 GHR and ATR

As explained in section 3.1.3, to model the heat transfer between the catalyst-filled pipelines where the inlet of GHR is, and the outlet of ATR, a slack variable Q_{GHR} is introduced to GHR. Then instead of a cross-connection between the two reactors, the reactors are connected, and an additional cooler is added to the flowsheet to simulate the heat that GHR receives from the ATR by cooling down the stream after the ATR with the same heat amount as GHR receives. Additionally, to ensure that the inlet cold stream can not have a higher temperature than the outlet hot stream, 2 additional constraints have been implemented in the model with an approach temperature of 25 °C. A simplified GHR and ATR connection figure is shown in fig. 5.

The modified version of the GHR and ATR model with the new connectivity is shown in fig. 6. The plot of distance, x, in the GHR reactor and the temperature of the hot and cold stream is shown in fig. 7.

Where the cold stream is the stream in the catalyst-filled pipelines, and the hot stream is the outlet stream of the ATR that gives off heat to the stream in the pipeline. Additional constraints to keep the temperature differences at the lower and outer bound of x have been added to the model as:

$$T_{ATR,out} - T_{GHR,out} \geq 25 \tag{4.1.34}$$

$$T_{postATR,out} - T_{GHR,in} \geq 25 \tag{4.1.35}$$

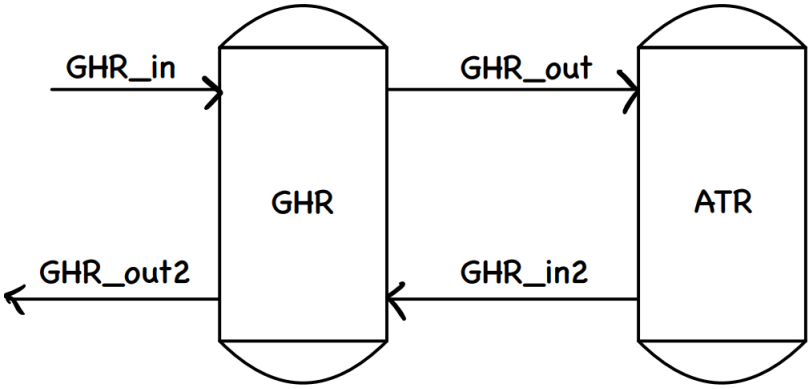

Figure 5: Simplified figure of the connectivity between GHR and ATR.

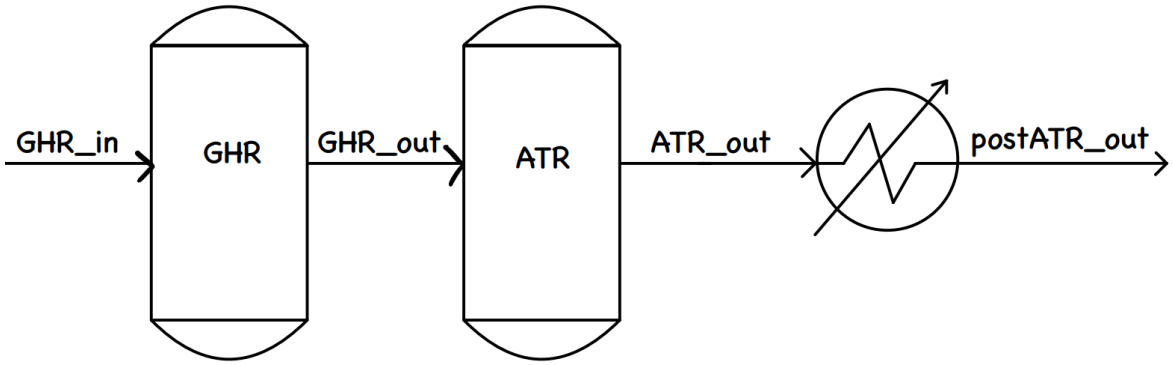

Figure 6: The modified version of GHR and ATR model.

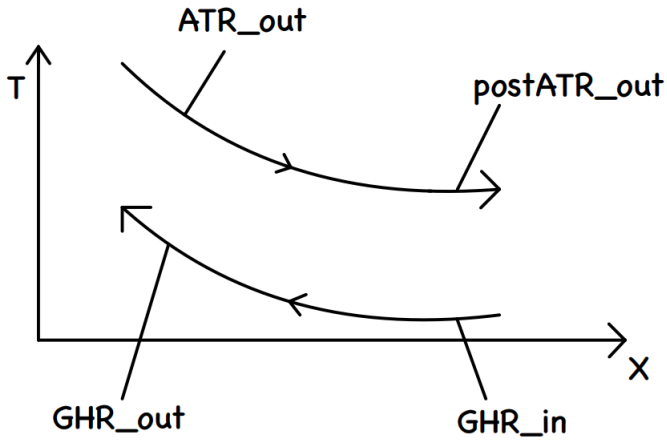

Figure 7: Heat exchanger temperature plot in the GHR.

where the right-hand side value of both inequalities has been set to an arbitrary value. Furthermore, another constraint to keep the heat added to the GHR, Q_{GHR}, and the heat

removed after ATR, $Q_{postATR}$, the same, another constraint has been added to the model as:

$$Q_{GHR} + Q_{postATR} = 0. \tag{4.1.36}$$

Note that both signs of the terms in eq. (4.1.36) are positive, as $Q_{postATR}$ is negative. It is also worth mentioning that the energy balance in the ATR contains a term for enthalpy change given by the oxygen feed.

5 Results

5.1 Case 1: Finalization of the model

The model was concluded to be finalized as the simulator found a feasible point that satisfied all constraints. The operating temperature of the GHR was set to be unbounded by an equipment specification constraint, and rather be bounded by a variable constraint of ±50 of its typical operating temperature. This means that 1 degree of freedom frees up, which allows the heat exchange inequalities to be satisfied, as the temperature set for the reactor may not satisfy the inequality. The optimizer then finds the operating point such that the hydrogen product stream is maximized. The mass balance is shown to be satisfied for every stream as well. The resulting mole stream and temperature for every stream of the finalization of the model are shown in table 3.

Table 3: Mole stream table of the finalized model.

Stream	T [K]	CH_4 [kmol h^{-1}]	H_2O [kmol h^{-1}]	H_2 [kmol h^{-1}]	CO [kmol h^{-1}]	CO_2 [kmol h^{-1}]
1	311.0	113.76	0.00	0.00	0.00	1.95
2	423.0	0.00	358.52	0.00	0.00	0.00
3	381.4	113.76	358.52	0.00	0.00	1.95
4	693.0	113.76	358.52	0.00	0.00	1.95
5	659.2	182.41	303.33	44.02	0.49	29.30
6	753.0	182.41	303.33	44.02	0.49	29.30
7	964.8	124.71	221.46	241.30	34.03	53.46
8	1323.0	0.71	268.46	442.28	160.96	50.53
9	778.0	0.71	268.46	442.28	160.96	50.53
10	523.0	0.71	141.20	569.54	33.69	177.79
11	313.0	0.71	141.20	569.54	33.69	177.79
12	313.0	0.00	141.06	0.00	0.00	0.00
13	313.0	0.71	0.14	569.54	33.69	177.79
14	313.0	0.007	0.001	568.97	0.34	1.78
15	313.0	0.71	0.14	0.57	33.36	176.01

It is worth noting that heavier hydrocarbons than methane are not mentioned in table 3, as it is constant from the initial stream until it enters the pre-reformer, where they become zero. The initially calculated stream of heavier hydrocarbons using the initial mole stream that was calculated in section 4 of 145.4 kmol h^{-1} with the composition found in table 1 is shown in table 4.

Table 4: Initial mole stream of heavier hydrocarbons than methane.

C_2H_6 [kmol h^{-1}]	C_3H_8 [kmol h^{-1}]	i-C_4H_{10} [kmol h^{-1}]	n-C_4H_{10} [kmol h^{-1}]	C_5H_{12} [kmol h^{-1}]
8.869	9.742	3.606	2.050	5.380

A table of the composition of all streams is shown in table 5. It is worth noting that at the end of the process, almost all methane and CO have converted, leaving only H_2, H_2O, CO_2 where the process condensate unit and the PSA unit, respectively remove the last two compounds.

Table 5: Stream mole% of the finalized model.

Stream	CH_4	H_2O	H_2	CO	CO_2	C_2H_6	C_3H_8	n-C_4H_{10}	i-C_4H_{10}	C_5H_{12}
1	0.783	0.000	0.000	0.000	0.013	0.061	0.067	0.025	0.014	0.037
2	0.000	1.000	0.000	0.000	0.000	0.000	0.000	0.000	0.000	0.000
3	0.226	0.712	0.000	0.000	0.004	0.018	0.019	0.007	0.004	0.011
4	0.226	0.712	0.000	0.000	0.004	0.018	0.019	0.007	0.004	0.011
5	0.326	0.542	0.079	0.001	0.052	0.000	0.000	0.000	0.000	0.000
6	0.326	0.542	0.079	0.001	0.052	0.000	0.000	0.000	0.000	0.000
7	0.185	0.328	0.357	0.050	0.079	0.000	0.000	0.000	0.000	0.000
8	0.0008	0.291	0.479	0.174	0.055	0.000	0.000	0.000	0.000	0.000
9	0.0008	0.291	0.479	0.174	0.055	0.000	0.000	0.000	0.000	0.000
10	0.0008	0.153	0.617	0.037	0.192	0.000	0.000	0.000	0.000	0.000
11	0.0008	0.153	0.617	0.037	0.192	0.000	0.000	0.000	0.000	0.000
12	0.000	1.000	0.000	0.000	0.000	0.000	0.000	0.000	0.000	0.000
13	0.0009	0.0002	0.728	0.043	0.227	0.000	0.000	0.000	0.000	0.000
14	0.000	0.000	0.996	0.0006	0.003	0.000	0.000	0.000	0.000	0.000
15	0.003	0.0007	0.003	0.158	0.835	0.000	0.000	0.000	0.000	0.000

Other essential variables worth reporting from the simulation are the heat required and recovered in each heat exchanger unit, the amount of oxygen needed in the ATR unit to satisfy the energy balance, and the hydrogen efficiency. Hydrogen efficiency is the amount of hydrogen in the interested stream divided by the sum of all hydrogen entering the process. Other essential variables are shown in table 6.

Table 6: Required oxygen, H_2 efficiency and heat required and recovered of the process in the finalized model.

Variable	Value	Unit
O_2	84.029	[kmol h^{-1}]
H_2 Eff.	0.799	[-]
Q_{prePR}	6.890	[GJ]
Q_{preGHR}	2.321	[GJ]
Q_{ghr_Q}	17.774	[GJ]
$Q_{postATR}$	-17.774	[GJ]
Q_{ITSR}	-12.621	[GJ]
$Q_{preCond}$	-6.396	[GJ]

5.2 Case 2: Studying the model by changing initial methane%

To test the model sensitivity, an important variable is chosen to adjust its initial values to see how certain important output variables will react to that change. In this case, the initial composition of methane was changed by $78.27\% \pm 10\%$ to see how final H_2 product stream, H_2 efficiency, required amount of O2, required heating and cooling resulted with varying initial condition. It is worth noting that, even though the composition of methane changes, the ratio between the other components keeps constant. This is done by applying eq. (5.2.1) for all components in the initial stream except methane.

$$x_{i,new} = \frac{x_{i,old} \cdot x_{\mathrm{CH_4},new}}{x_{\mathrm{CH_4},old}}, \tag{5.2.1}$$

where $x_{i,old}$ and $x_{i,new}$ are the composition of component i, before and after the change in the composition of methane and component i, is all of the nonzero components in the initial stream except methane. $x_{\mathrm{CH_4},old}$ and $x_{\mathrm{CH_4},new}$ are the old and new composition of methane in the initial stream. The resulting plot where methane% is plotted against H_2 in the product stream, H_2 efficiency, required amount of O_2 in the ATR unit, required heating and cooling is shown in fig. 8, fig. 9 and fig. 10, fig. 11 and fig. 12 respectively.

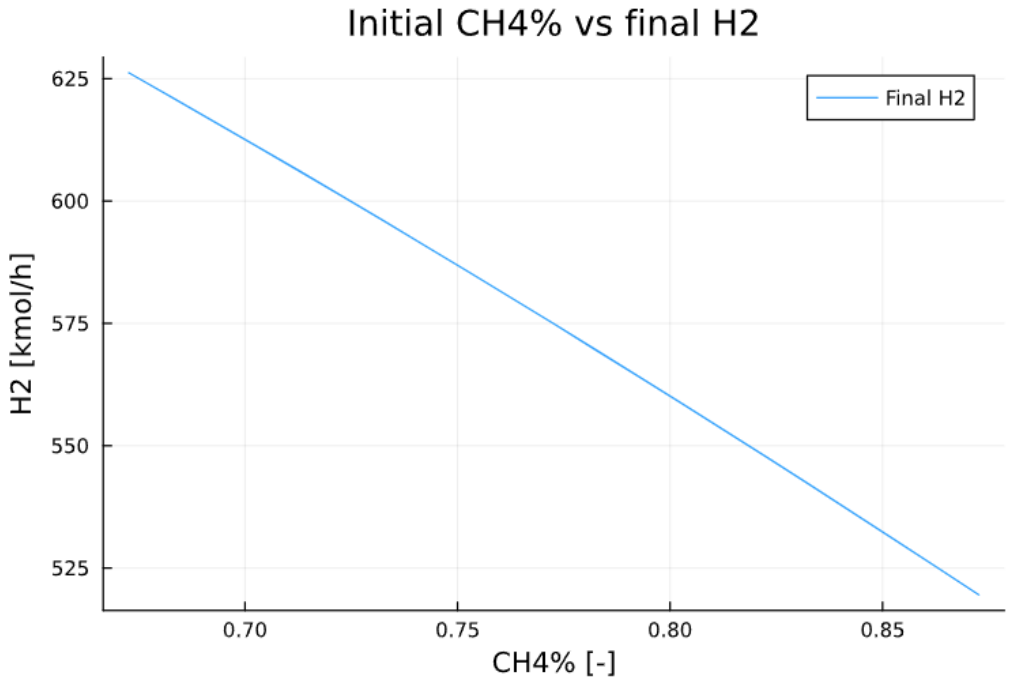

Figure 8: Change in initial CH_4 composition plotted against H_2 in the product stream.

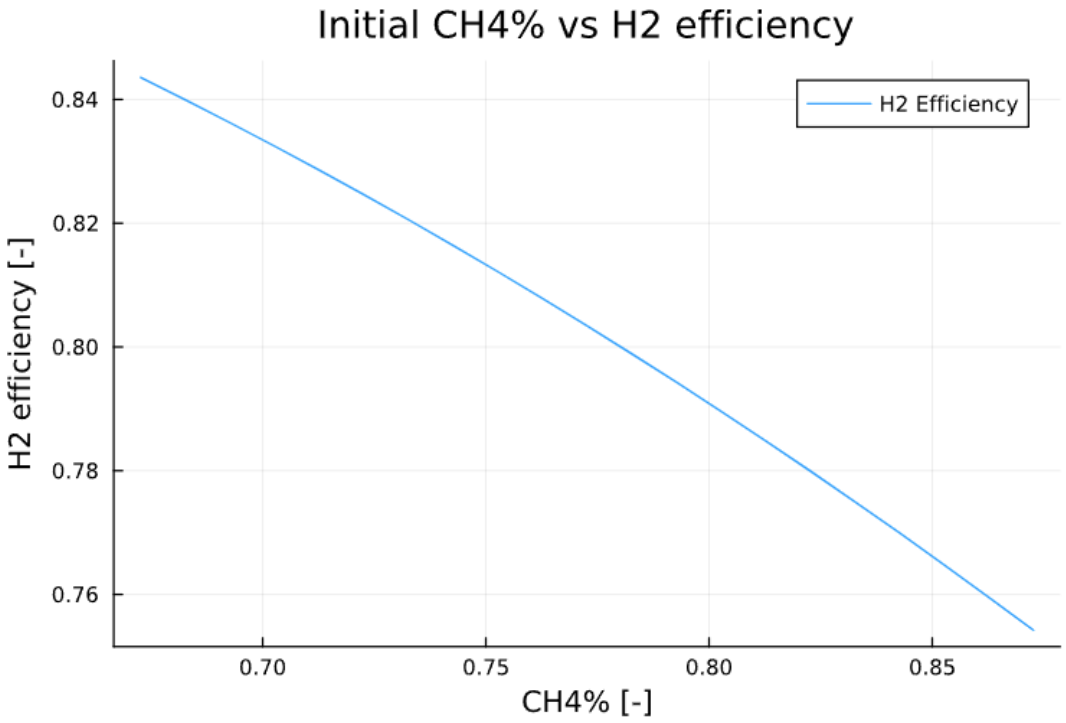

Figure 9: Change in initial CH_4 composition plotted against H_2 efficiency.

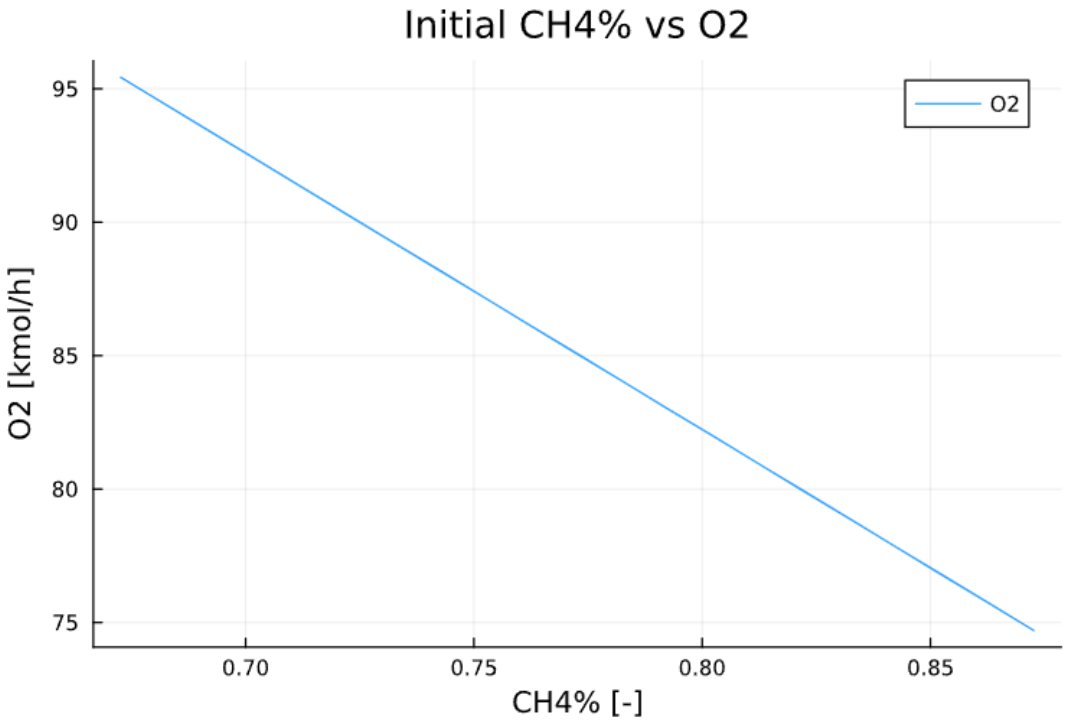

Figure 10: Change in initial CH_4 composition plotted against O_2 required in the ATR unit.

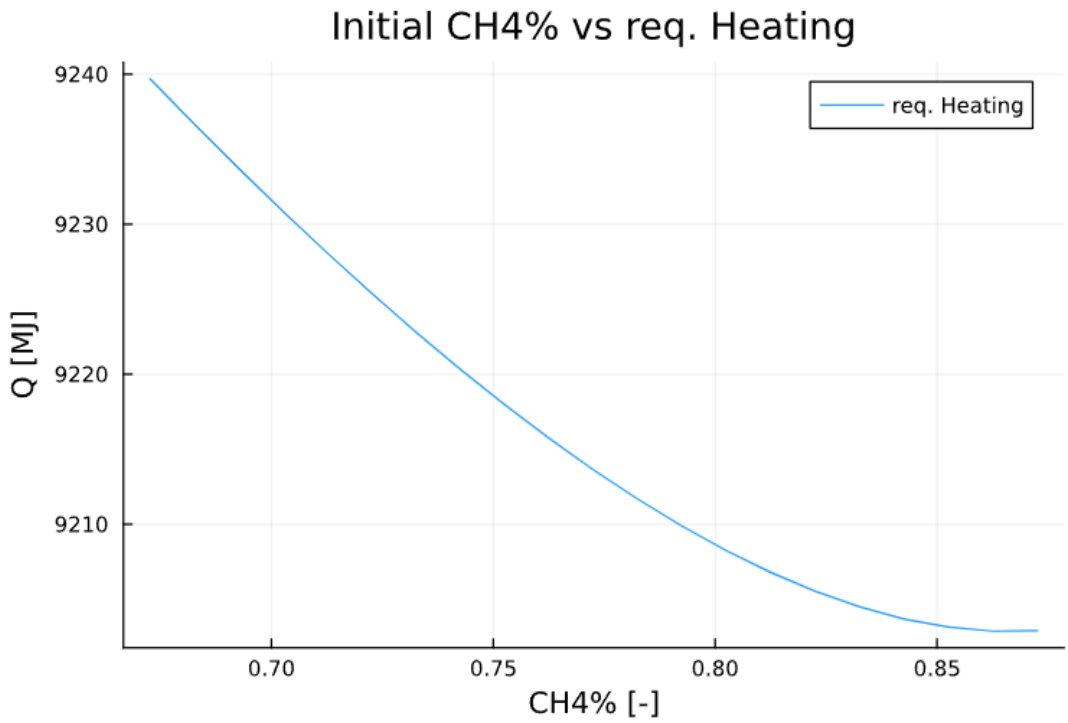

Figure 11: Change in initial CH_4 composition plotted against required amount of heating in the process.

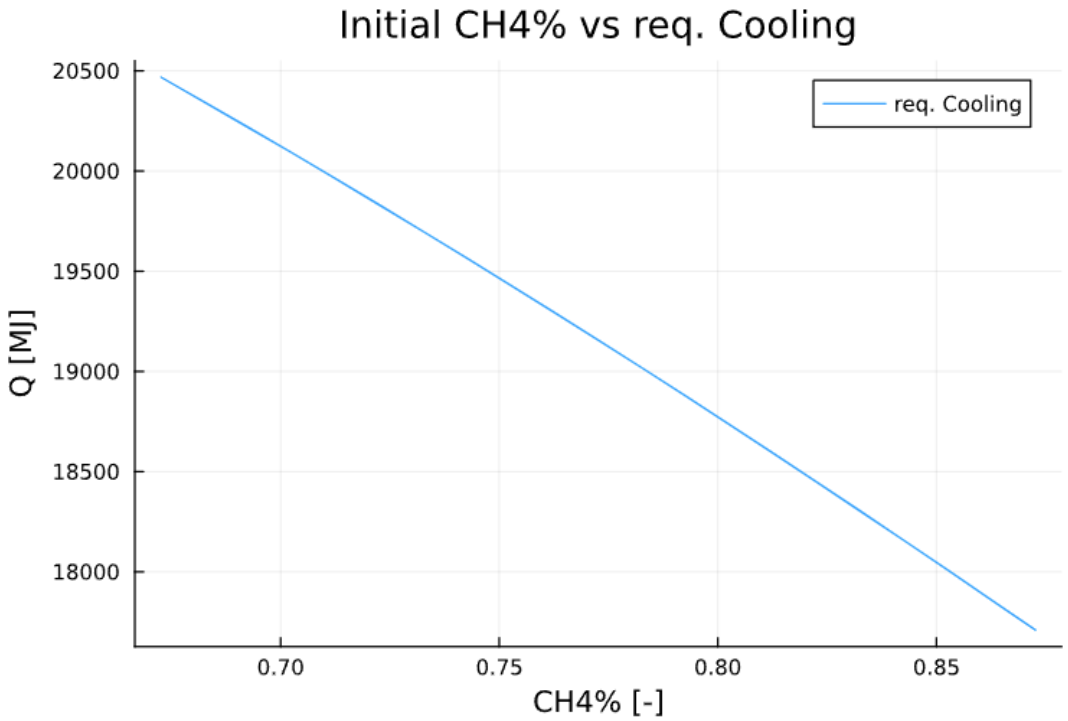

Figure 12: Change in initial CH_4 composition plotted against required amount of cooling in the process.

5.3 Case 3: Studying the model by changing the steam to carbon ratio

The following variable to vary to see the model's sensitivity is the steam-to-carbon ratio, which is one of the set initial values. In other words, it sets the amount of H_2O fed into the process. In the finalized model, this variable is set to a value of 2.5. The steam-to-carbon ratio range of $[1.0, 3.0]$ will be studied in this case. The same output variables as case 2 shown in section 5.2 will be used. In other words, in case 3, the model will be studied by varying the steam-to-carbon ratio and plotting it against H_2 in the product stream, H_2 efficiency, O_2 required in the ATR unit and required amount of heating and cooling in the process. Varying amount of steam in the inlet stream plotted against H_2 in the product stream, H_2 efficiency, O_2 required in the ATR unit. The necessary amount of heating and cooling is shown in fig. 13, fig. 14, fig. 15 and fig. 16, respectively.

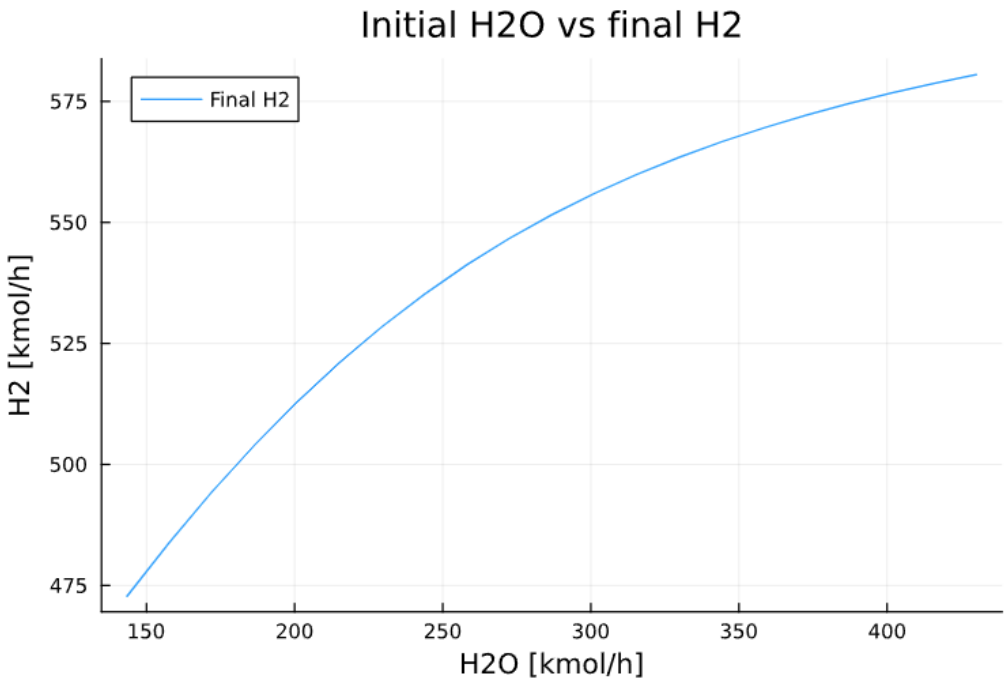

Figure 13: Change in H_2O at inlet plotted against H_2 in the product in stream.

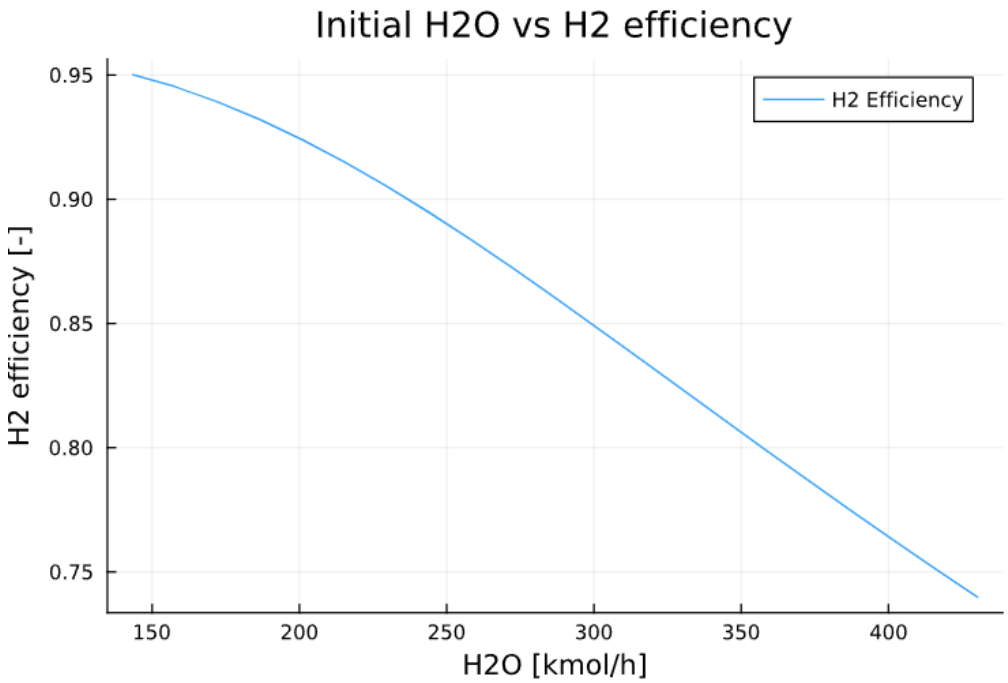

Figure 14: Change in H_2O at inlet plotted against H_2 efficiency.

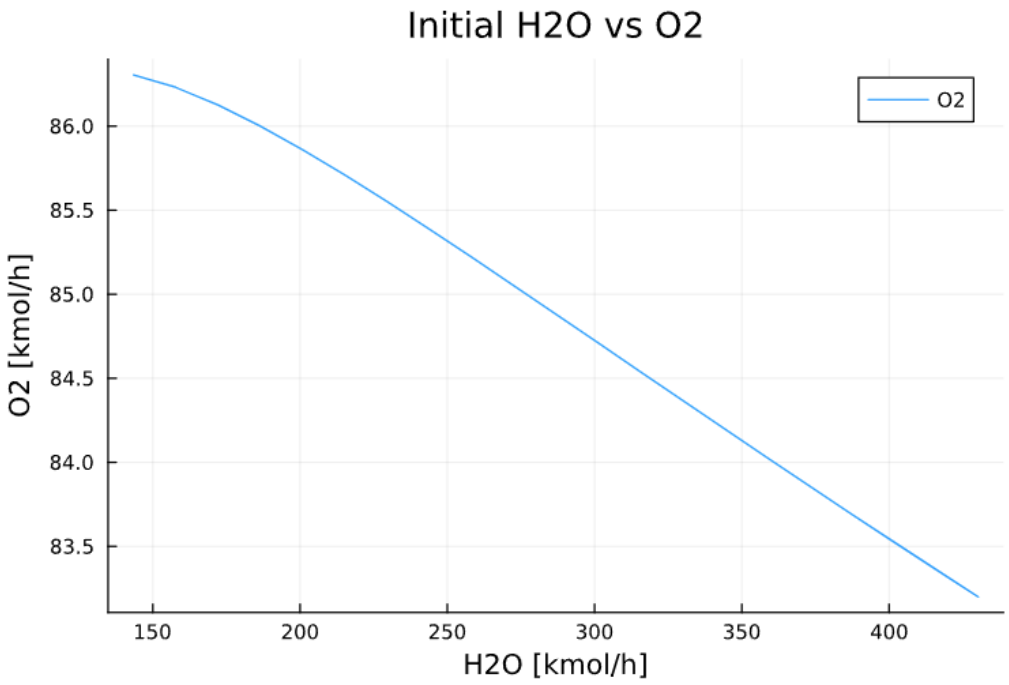

Figure 15: Change in H_2O at inlet plotted against required amount of O_2 in the ATR unit.

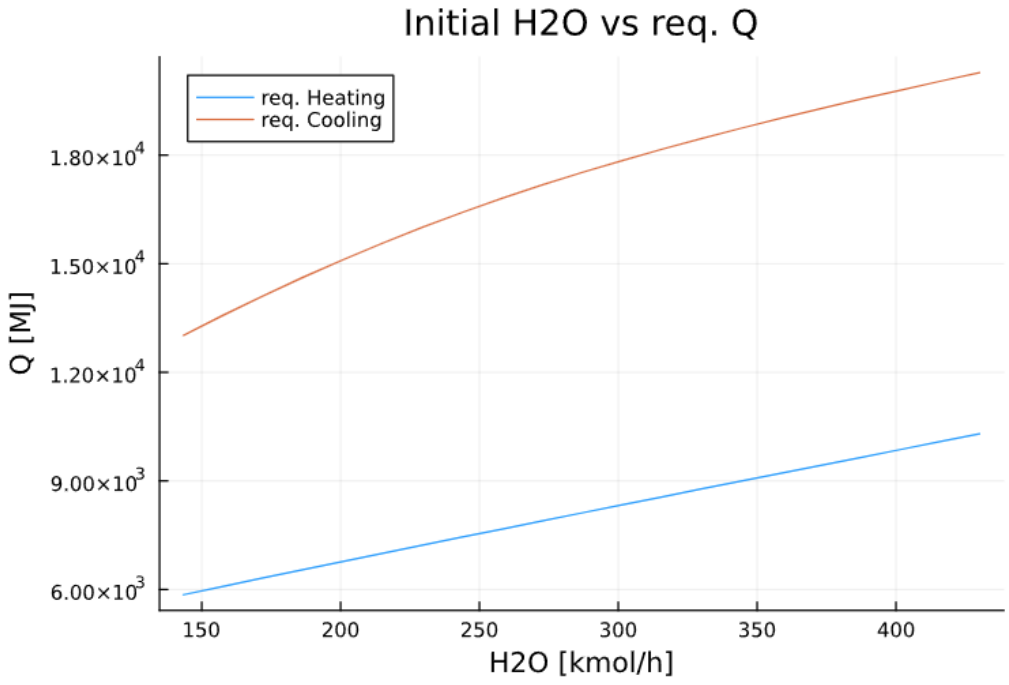

Figure 16: Change in H_2O at inlet plotted against required amount of heating and cooling in the process.

6 Discussion

6.1 Case 1: Finalization of the model

This discussion will be based on the results from case 1, which is shown in section 5.1. Table 3 shows that the temperature of each stream is within an acceptable level of bounds from the typical operating temperature reported from various literature. The resulting amount of H_2 approximately $568.97\,\mathrm{kmol\,h^{-1}}$. All components at the inlet containing hydrogen atoms are potential atoms that become H_2. Two main components carry hydrogen atoms into the process after the pre-reformer unit, which is CH_4 and H_2O. As almost all CH_4 converts, the main exiting components containing hydrogen atoms are either H_2 or H_2O. The mole stream table shown in table 3 shows that majority of the exiting component containing hydrogen atoms are H_2, which is desired. However, the remaining H_2O that is being removed at the process condensate unit can be recycled into the saturator after being heated up. This will lead to all hydrogen atoms in the feed exits as H_2 product.

From the composition table of the streams in the process shown in table 5, it can be observed that after the pre-reforming process, 30% of H_2O is being used up. This may lead to the following reactors not have enough H_2O reactant which leads to the equilibrium not being shifted enough towards right as it could have been. In the case of CH_4, almost all converts as after the GHR and ATR units, it becomes only 0.8% of the stream. However, in the case of CO, where the majority should be converted in the ITSR unit, it leaves the reactor as 3.7% of the outlet stream. This could be because the reactor did not have enough steam to shift the equilibrium to the right. To fix this, another inlet stream of steam could be added to the process before the ITSR unit to ensure maximal conversion of CO.

It is hard to comment on how required O_2, H_2 efficiency, and different required heating and cooling in the process are good values. However, there seems to be a possibility to run a heat pinch analysis and see if there are any heaters and coolers that can exchange heat to reduce the need for external energy sources. This requires that the temperature range of the heaters and coolers are within ranges that can exchange. In other words, the temperature range of the cooler can not be lower than the temperature range of the matching heater in order to exchange heat. The required amount of O_2 fed into the ATR unit is also relatively high, as for every 2 moles of CH_4 in the feed; the process requires approximately 1 mole of O_2. The scope of this project does not include sources of pure O_2, but with methods like electrolysis or cryogenic distillation, this will be a significant cost to operate the system.

6.2 Case 2: Studying the model by changing initial methane%

For discussing case 2, results shown in section 5.2 will be used. In case 2, an important variable, initial CH_4%, will be varied to study how the model responds to it, where the output variables were H_2 product stream, H_2 efficiency, O_2 required in the process, and required heating and cooling in the process. In summary, the output was insensitive to the input change and showed strong linear relations. However, it is hard to explain the reason behind linear response due to the large number of equations in the system. From the plots

shown in fig. 8, fig. 9, fig. 10, fig. 11 and fig. 12, that are being discussed, it can be concluded that the system is running stable.

6.2.1 Initial methane% vs hydrogen product stream

Figure 8 shows strong linear relations, and shows a significant change. CH_4% varies from ±10% of its value from the finalized model of 78.27%, while H_2 in the product stream seems to vary from approximately 525 - 625 kmol h^{-1}, which is 575 ± 50kmol h^{-1}, approximately ±10%. From these numbers, it can be concluded that hydrogen in the product stream is relatively sensitive to varying CH_4% as both change in input and resulting output has the same magnitude. It is worth noting that increasing CH_4% at the inlet leads to less H_2 produced. This could be since when varying the CH_4% at the inlet, the total mole stream is set as constant, while the composition of other hydrocarbons changes with changing CH_4% in an inverse proportional way. This leads to also more H_2O added since it is based on the hydrocarbons in the feed. In other words, when increasing CH_4%, there will be less of the other heavier hydrocarbons, which leads to fewer hydrogen atoms entering the process.

6.2.2 Initial methane% vs hydrogen efficiency

Figure 9 shows that the response is slightly quadratic, and hydrogen efficiency is relatively insensitive to change in initial CH_4%. From the plot, H_2 efficiency seems to have a nominal value of approximately 0.85 with a variations of ±5% with a input change of ±10%. Notice that H_2 efficiency is decreasing with increasing CH_4%. The same reason as explained in section 6.2.1 can be used where increasing CH_4% in the feed decreases the number of hydrogen atoms entering the process.

6.2.3 Initial methane% vs O2

Figure 10 shows that the relation between initial CH_4% and O_2 is also linear, with O_2 being relatively sensitive to change in CH_4% as the change in the output is approximately same the as the magnitude in input change. It is observed in the plot that with increasing CH% in the feed, the required amount of O_2 also decreases; also, the two variables are proportional. This relation will be important when considering an economic trade-off since decreasing O_2 by increasing CH_4% will increase the profit, but at the same time, increasing CH_4% will also lead to less hydrogen produced.

6.2.4 Initial methane% vs req. heating and cooling

Figure 11 shows that the required amount of heating is linear until approximately 0.85% of initial, CH_4, then it shows a trend to a value of about 9200 MJ. It is also insensitive to the initial CH_4% change as it has a varying output value of ±0.2% of its nominal value. Furthermore, fig. 12 shows that the required amount of cooling in the process has strong linearity throughout the range of changing values of initial CH_4%, with a relatively insensitive response as the output value has a variation of ±6.5% of its nominal value.

6.3 Case 3: Studying the model by changing the steam-to-carbon ratio

Results from case 3 shown in section 5.3 will be used to discuss the last case. In case 3, the steam-to-carbon ratio was set to a range from $[1.0, 3.0]$. Steam-to-carbon is a variable that set the amount of steam that adds to the process initially. In summary, the output variables that were studied were less sensitive than the results from case 2, shown in section 5.2. Also, the relations were a bit more nonlinear than in case 2, but still relatively linear. The horizontal axis was set to the amount of H_2O in the initial stream instead of the steam-to-carbon ratios as it is easier to see the relations between the output and the change in initial conditions.

6.3.1 Steam-to-carbon ratio vs hydrogen product stream

Figure 13 shows a curve, where H_2 product stream increases with increasing steam added in the process. This makes sense at more H_2O in the process introduces more hydrogen atoms in the system, and it shifts the equilibrium to the right which leads to more conversion. The H_2 variable in the product stream is also relatively insensitive to H_2O change at the inlet as the input varies with $\pm 100\%$ while the output changes only by approximately $\pm 10\%$ of its nominal value.

6.3.2 Steam-to-carbon ratio vs hydrogen efficiency

Figure 14 shows a declining linear trend, with relatively insensitive response to input variations as the output, H_2 efficiency, only changes about $\pm 10\%$ from its nominal value where the input varies with $\pm 100\%$. It is worth noting that with increasing steam-to-carbon ratio, H_2 product stream increases, but H_2 efficiency decreases. This means that even though H_2 product increases, amount of unreacted H_2O also increases. Without an economical analysis, it is hard to conclude the optimal steam-to-carbon ratio as too high ratio can lead to more expensive operation due to unnecessary heating of reactants and more expensive process equipment sizing. On the contrary, too low steam-to-carbon ratio leads to less conversion in the reactors and less H_2 product which leads to loss in potential profit.

6.3.3 Steam-to-carbon ratio vs O2

The plot where varying steam-to-carbon ratio plotted against the required amount of O_2 is shown in fig. 15. The plot shows a slight nonlinear response initially, but the majority is linear. The results also show that the O_2 is relatively insensitive to the initial H_2O change as the output has a change of approximately $\pm 2.5\%$ of its nominal value. However, it is important to observe that the plot has a decreasing trend, which is good as O_2 is an expensive reactant. In other words, by adding more H_2O to the process, profit will increase as H_2 in the product stream increases and the need for the expensive reactant O_2 decreases. The decrease can be explained by the fact that if the system is saturated with steam, there can be more unreacted steam in the reactors, which can "absorb" energy, thus requiring less

enthalpy contribution from oxygen combustion.

6.3.4 Steam-to-carbon ratio vs. req. Heating and Cooling

The plot of varying steam-to-carbon ratios against the required heating and cooling in the process is shown in fig. 16. The plots show that heating and cooling increase with increasing H_2O. Both output variables are relatively sensitive to change in input, as both out increase by approximately 50%, while other outputs only increased by $5 - 10\%$. Increasing cooling can be positive as it does not require as much energy as heating. Since the process is based offshore, plenty of ocean water can be used as a coolant. But an increasing amount of required heating can be more troublesome as it requires more energy and can potentially be a huge factor in evaluating the economic analysis. Still, it also requires more power in the system. As more energy is recovered than required in the system, it is important to create a heat exchanger network, where the heaters and coolers exchange heat with each other to reduce the need to add more energy to the system. It is hard to conclude whether increasing H_2O will increase profit without doing an economic analysis as it increases H_2.

7 Conclusion

For case 1, where the finalized model was studied, the resulting streams of the model were close to the reported version of the process that this model was based on [13]. The operating temperatures of the reactors were within an acceptable level of bounds, and after each reactor, showed good conversion results. It is important to note two things in the finalized model. Firstly, it is assumed to be 1500 kPa in the reactors, while no compressors or turbines were implemented in the system. Second, the impurities of the CO_2 stream in the PSA unit is not checked to be in bounds for regulations when it comes to allowed impurities when storing captured CO_2. To improve this model, these considerations need to be taken into account.

Case 2 showed that increasing initial CH_4% leads to a decrease in all output values. As explained in section 6.2.1, increase in CH_4% ultimately leads to fewer hydrogen atoms added to the system, which leads to less hydrogen exiting the system. Fewer reactants will give less product, and not enough H_2O in the system (non-saturated) can lead to the reactions in the reactors not fully converting at the given operating conditions. And also decrease in reaction happening will reduce the necessary enthalpy input from combusting oxygen, thus leading to less oxygen needed in the system. In reality, the component mole stream of heavier hydrocarbons changes but is not based on CH_4, so it can be hard to predict the output. That is why it will be essential to implementing a robust plantwide control structure that can counteract the disturbances (change in hydrocarbons) to ensure maximum profit or minimal energy cost.

Lastly, case 3 showed that steam-to-carbon ratio may be important for the process economics as, increasing the steam-to-carbon ratio increased H_2 product stream while decreasing the need for oxygen. These two observations will increase profit, but the necessary amount of heat also increases. Without a complete heat exchanger network and economic analysis, it is hard to conclude at which point increasing the steam-to-carbon will positively contribute to profit.

In summary, from the 3 cases that were done, the steady-state model developed in this project can be concluded to be stable and robust. The system runs stably for changes of important initial values. This model is concluded to be finalized for this project and is ready to be used for further analysis. Additionally, the code used for the model is backed up with GitHub, a version control system [25].

8 Further work

Although a lot was done in this project to develop the existing model as SUBPRO, there is more to be done to conclude the model as finished. Firstly, there are still a few things to implement to the model before it can be used for further analysis. As mentioned in the discussion section, pressure drops were not implemented in the process yet; At the same time, the gas enters the system at 3000 kPa, while the reactors operate at 1500 kPa. Product and flue gas stream should also be compressed for transportation. This process will be energy intensive and costly, and will be an important factor when doing a feasibility analysis. To minimize the loss in profit, a recycle stream from the process condensate to either feed or before the reactors can be implemented to reduce the need for an external steam source and ensure that the inlet before the reactors are saturated with steam to ensure maximum conversion. Note that this stream from the process condensate most likely needs to heat up and compress to match the stream conditions it adds to.

Another implementation to reduce loss in profit is a heat exchanger network. As long as the hot and cold streams can match, a heater and a cooler can be checked together to reduce the need for heating in the system. It is more important to focus on the cold streams that need heating since the hot streams that need cooling can be cooled down using ocean water. Since the process operates offshore, surrounded by ocean water, it can be considered free.

As for now, the process has ideal split factors, both in the process condensate and in the PSA unit. For the case of the process condensate unit, the split factor can be implemented mathematically by calculating thermodynamic relations with vapor-liquid phases. It is more complicated for the PSA unit as it is advanced adsorption happening in the tanks. For further work, the split factor in the PSA unit will be based on numbers from different sources and reports. Also, the composition of the flue gas from the PSA unit will be controlled to be within the bounds of CO_2 capture and storage regulations. When all that is implemented, the next goal is then to build the model in such a way that it is more modular, in other words, a good user interface where it will be easy and intuitive to run the model in different ways, such as switching between different objective values.

A robust plantwide control structure is needed to ensure that the model operates ideally for most disturbances. When this is implemented, and the model is concluded to be finalized, it can be used for feasibility analysis. In addition, to perform such an analysis, the sizing of each unit also needs to be calculated to calculate the final investment. This sum will be the required sum to pay off from income before the process profits.

References

[1] Tuong-Van Nguyen, Brian Elmegaard, Leonardo Pierobon, Fredrik Haglind, and Peter Breuhaus. Modelling and analysis of offshore energy systems on north sea oil and gas platforms. In *53rd International Conference of Scandinavian Simulation Society*, 10 2012.

[2] Rob West and Bassam Fattouh. The energy transition and oil companies' hard choices, 2019. URL https://www.oxfordenergy.org/wpcms/wp-content/uploads/2019/07/The-Energy-Transition-and-Oil-Companies-Hard-Choices-Energy-Insight-51.pdf.

[3] Hannah Ritchie, Max Roser, and Pablo Rosado. Energy, 2022. URL https://ourworldindata.org/energy-mix.

[4] European Commission. 2050 long-term strategy, 2022. URL https://climate.ec.europa.eu/eu-action/climate-strategies-targets/2050-long-term-strategy_en.

[5] Chunshan Song. *Hydrogen and Syngas Production and Purification Technologies*, pages 1 – 13. Wiley, 11 2009. ISBN 9780470561256. doi: 10.1002/9780470561256.ch1.

[6] U.S. Energy Information Administration. How is hydrogen produced?, 2022. URL https://www.eia.gov/energyexplained/hydrogen/production-of-hydrogen.php.

[7] Robert Howarth and Mark Jacobson. How green is blue hydrogen. *Energy Science and Engineering*, 9, 08 2021. doi: 10.1002/ese3.956.

[8] SUBPRO. About subpro, 2022. URL https://www.ntnu.edu/web/subpro/aboutsubpro.

[9] Jorge Nocedal and Stephen J. Wright. *Numerical Optimization*. Springer, New York, NY, USA, 2e edition, 2006. page 2.

[10] Sigurd Skogestad. *Prosessteknikk, masse- og energibalanser*. Fagbokforlaget, 3rd edition, 2014. ISBN 9788251924573. pages 72-74.

[11] Sigurd Skogestad. *Prosessteknikk, masse- og energibalanser*. Fagbokforlaget, 3rd edition, 2014. ISBN 9788251924573. pages 88-94.

[12] Seongkyu Yoon, Shaun Galbraith, Bumjoon Cha, and Huolong Liu. Chapter 5 - flowsheet modeling of a continuous direct compression process. In Ravendra Singh and Zhihong Yuan, editors, *Process Systems Engineering for Pharmaceutical Manufacturing*, volume 41 of *Computer Aided Chemical Engineering*, pages 121–139. Elsevier, 2018. doi: https://doi.org/10.1016/B978-0-444-63963-9.00005-1. URL https://www.sciencedirect.com/science/article/pii/B9780444639639000051.

[13] Robert Hardy and Neha Vijh. Accelerating the Path to Net Zero with Blue Hydrogen: A Route to Achieving Best-In-Class Environmental Performance and Economics. *Abu*

Dhabi International Petroleum Exhibition and Conference, Day 3 Wed, November 02, 2022, 10 2022. doi: 10.2118/210888-MS. URL https://doi.org/10.2118/210888-MS.

[14] Thomas S. Christensen. Adiabatic prereforming of hydrocarbons — an important step in syngas production. *Applied Catalysis A: General*, 138(2):285–309, 1996. ISSN 0926-860X. doi: https://doi.org/10.1016/0926-860X(95)00302-9. URL https://www.sciencedirect.com/science/article/pii/0926860X95003029.

[15] Y. Shirasaki and I. Yasuda. 12 - membrane reactor for hydrogen production from natural gas at the tokyo gas company: a case study. *Woodhead Publishing Series in Energy*, 2: 487–507, 2013. doi: https://doi.org/10.1533/9780857097347.2.487. URL https://www.sciencedirect.com/science/article/pii/B9780857094155500123.

[16] Rupam Mukherjee and Shilpa Singh. Evaluating hydrogen rich fuel gas firing, 2021. URL digitalrefining.com/article/1002591/evaluating-hydrogen-rich-fuel-gas-firing#.Y40CjXbMJPY.

[17] Dr. Max Appl. *Process Steps of Ammonia Production*, chapter 4, pages 65–176. John Wiley & Sons, Ltd, 1999. ISBN 9783527613885. doi: https://doi.org/10.1002/9783527613885.ch04.

[18] Laura Pellegrini, Giorgia Guido, and Stefania Moioli. Design of the co2 removal section for psa tail gas treatment in a hydrogen production plant. *Frontiers in Energy Research*, 8, 05 2020. doi: 10.3389/fenrg.2020.00077.

[19] Rafael M. Siqueira, Geovane R. Freitas, Hugo R. Peixoto, Jailton F. do Nascimento, Ana Paula S. Musse, Antonio E.B. Torres, Diana C.S. Azevedo, and Moises Bastos-Neto. Carbon dioxide capture by pressure swing adsorption. *Energy Procedia*, 114: 2182–2192, 2017. ISSN 1876-6102. doi: https://doi.org/10.1016/j.egypro.2017.03.1355. URL https://www.sciencedirect.com/science/article/pii/S1876610217315382. 13th International Conference on Greenhouse Gas Control Technologies, GHGT-13, 14-18 November 2016, Lausanne, Switzerland.

[20] Johnson Matthey. Lch process for the production of blue hydrogen, 2022. URL https://matthey.com/documents/161599/474986/26367+JM+LCH+Process+-+Production+of+Low+Carbon+Hydrogen+TP+%28screen%29+13.pdf/71bb11a0-47ce-e609-412b-0678b1b4e5da?t=1654695668629.

[21] Eva K.Hallanda, Van Phama, Fridtjof Riisa, and Ann-Helen Hansena. Co2 for eor combined with storage in the norwegian north sea, 2019. 14th International Conference on Greenhouse Gas Control Technologies, GHGT-14.

[22] Norsk Petroleum. Troll, 2021. URL https://www.norskpetroleum.no/fakta/felt/troll/.

[23] JuMP. Nonlinear modeling, 2022. URL https://jump.dev/JuMP.jl/stable/manual/nlp/.

[24] COIN-OR. Ipopt: Documentation, 2022. URL https://coin-or.github.io/Ipopt/.

[25] Yoonsik Oh. Github repository for the code used in the specialization project, 2022. URL https://github.com/yoonsiko/Specialization/tree/master/Specialization.

[26] Jorge Nocedal and Stephen J. Wright. *Numerical Optimization*. Springer, New York, NY, USA, 2e edition, 2006. pages 320-321.

A Optimality conditions

There are mathematical expressions known as optimality conditions to check if the solution given by the optimization algorithm indeed is the optimal point [9]. Karush-Kuhn-Tucker (KKT) conditions can verify if the solution is the optimal point, where the solution x^* is a local minima if there exists a Lagrange multiplier λ^*, such that the following conditions are satisfied at (x^*, λ^*) [26]:

$$\nabla_x \mathcal{L}(x^*, \lambda^*) = 0, \tag{A.0.1}$$
$$c_i(x^*) = 0, \quad \forall i \in \mathcal{E}, \tag{A.0.2}$$
$$c_i(x^*) \geq 0, \quad \forall i \in \mathcal{I}, \tag{A.0.3}$$
$$\lambda_i^* \geq 0, \quad \forall i \in \mathcal{I}, \tag{A.0.4}$$
$$\lambda_i^* c_i(x^*) = 0, \quad \forall i \in \mathcal{E} \cup \mathcal{I}, \tag{A.0.5}$$

where $\mathcal{L}(x, \lambda)$ is the Lagrangian function and is defined as

$$\mathcal{L}(x, \lambda) = f(x) - \sum_{i \in \mathcal{E} \cup \mathcal{I}} \lambda_i c_i(x). \tag{A.0.6}$$

The KKT-conditions does not sufficiently characterize an optimum alone. Two additional conditions also needs to hold for a solution to be guaranteed a solution. The first one is the Linear Independence Constraint Qualification (LICQ) and it requires that all of the gradients of the active constraints are linear independent of each other at the solution. The second additional condition is the second order sufficient condition and it requires the Hessian of the Lagrangian is positive semi-definite at the solution.